

**A CENTER FED MULTI-BAND ANTENNA FOR SIMULTANEOUS SATELLITE COMMUNICATION AT C AND KU BANDS**

R. J. Bauerle, G. Gothard, A. Vergamini  
 Harris Corporation  
 Melbourne, FL 32902-0037

**ABSTRACT**

*As the Navy requires increased data throughput via satellite communications at sea, the need for a vessel based SATCOM multi-band antenna operating at both C and Ku-bands is on the rise. The design of a compact, high performance, simultaneous C and Ku-band antenna and feed presents many technical challenges. Such challenges include mechanical packaging of the feed components with short focal length optics, broadband axial ratio that is less than 0.75 dB, and broadband high efficiency. This paper describes the design and testing of a multi-band coaxial antenna subsystem as part of the Navy Commercial Broadband Satellite Program (CBSP). The subsystem includes capability to switch among linear and circular polarization at C-band as well as adjustable linear polarization at Ku-band. Both software simulations and test data are presented for the antenna performance.*

**1. INTRODUCTION**

The Commercial Broadband Satellite Program (CBSP) is sponsored by the Department of the Navy Research, Development and Acquisition (ASN RDA) with a primary goal of providing nearly 50 ships with significant upgrades to existing satellite terminals. Navy vessels that currently have the capability for INMARSAT B HSD or Commercial Wideband Satcom Program (CWSP) services and achieve throughput of approximately 2.0 MB/s will be upgraded to throughput of over 20.0 MB/s if equipped with the CBSP Force Level Variant (FLV) terminal. Such services include broad band internet and e-mail access for all onboard with the purpose of improving soldier welfare and morale.

In addition to the large increase in throughput, the Navy needs expedited replacement of the existing terminals. Therefore the rapid design and prototype of the antenna subsystem and feed, a crucial component of the CBSP FLV terminal, is needed. The requirements of such an antenna and feed are summarized in Table 1. They were derived from many different system requirements including the desired throughput and anticipated tracking and stabilization; the stabilization was achieved via a 3-axis positioner and servo control hardware. The details of such derivation will not be included here.

TABLE 1

CBSB FLV ANTENNA SUBSYSTEM REQUIREMENTS

Description	Requirement
C-band frequency	3.7-4.2 GHz Rx, 5.85-6.425 GHz Tx
Ku-band frequency	10.95-12.75 GHz Rx, 13.75-14.50 GHz Tx
Simultaneous Operation	C&Ku bands: Tx-pol1, Rx-pol2
C and Ku band Aperture Efficiency	65% worst case over Tx, Rx bands
C-band Polarization	co-pol can be one of: RH, LH, V, H
Ku-band Polarization	co-pol can be one of V, H
C-band Gain	Rx:37.9 dBi, Tx:41.8 dBi
Ku-band Gain	Rx:47.2 dBi, Tx:49.2 dBi
C and Ku band Side Lobes	MIL-STD-188-164A [1]
C-band Axial Ratio	Tx 0.75 dB
C and Ku band XPD	Tx and Rx 30 dB

The simultaneous operation requirement refers to “pol1” being among any of the co-polarizations listed in the table and “pol2” also among those co-polarizations listed but always orthogonal to “pol1”. There is no polarization re-use requirement for the CBSP FLV antenna subsystem within a given band.

In addition to the requirements in the above table, the antenna and feed need to be as compact and as low mass as possible for efficient use of the ship’s space. Tight packaging as well as high efficiency requirements make designing this antenna very challenging. The design presented in this paper is a unique variant of a center fed coaxial design that allows efficient simultaneous dual-band use of the main reflector surface. The design process involved analysis and design of the optics and waveguide components with the most up to date commercially available software. Such analysis was used to significantly reduce the number of design iterations needed prior to a production-ready design

**2. ANTENNA AND FEED DESIGN**

Figure 1 shows a block diagram of the CBSP FLV antenna sub system. The optics is comprised of a ring-focus main and sub-reflector to allow a high efficiency and compact design. All of the components were developed by the Harris team with the exception of the Ku-band OMT and the motor that rotates internal parts of the C-band polarizer which were commercially available parts. Only the Harris developed parts will be described in this paper.

Figure 2 shows a 3-D drawing of the feed excluding the main and sub reflectors. A dielectric insert exists in the Ku-band portion of the feed and is needed to improve the return loss and isolation of the dual-band aperture. Figure 3 shows a 2D drawing of the same geometry with the addition of the sub reflector and its support. This drawing shows the internal features of the feed. The length from the Ku-band OMT common port to the horn aperture is shown indicating the size of the feed. All other sections of this drawing are to scale.

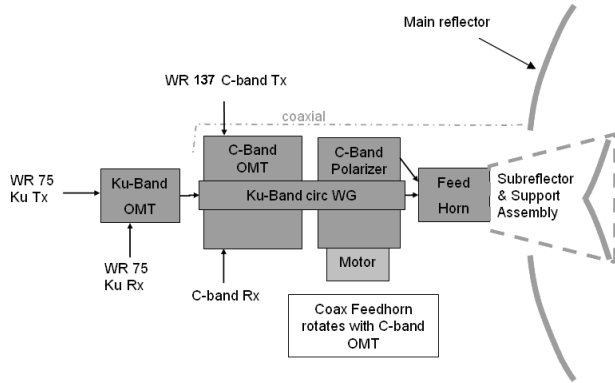


Figure 1 Antenna subsystem block diagram

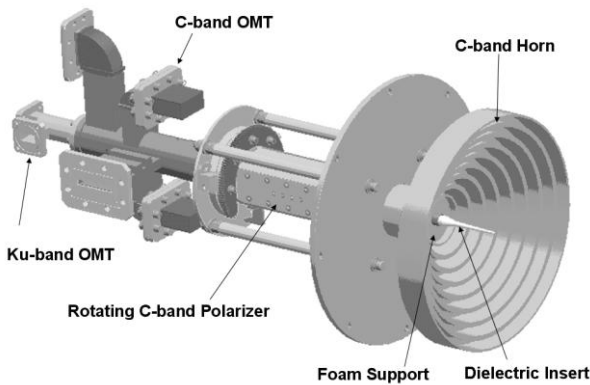


Figure 2 3D-drawing of the feed horn and waveguide components

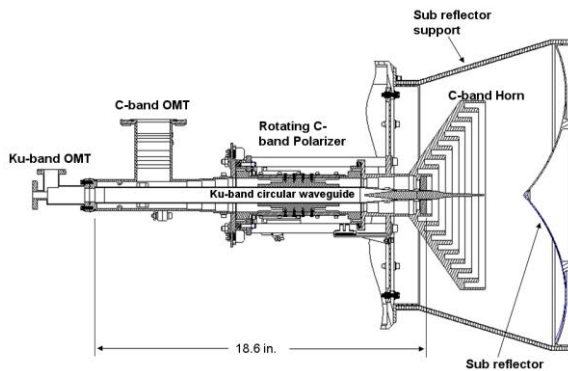


Figure 3 2D-drawing of feed horn and waveguide components

### A. Main and Sub Reflector Design

The antenna optics are comprised of a main and sub-reflector

in a displaced axis-Grigorian, or ring-focus, type design [2]. The reflector shapes were derived with an antenna shaping code as described in the reference. The ring-focus reflector antenna has a focal ring instead of the typical focal point of a parabolic reflector. This is accomplished by splitting a two-dimensional parabola, displacing the axis by some offset amount, then revolving to form a three-dimensional surface. Because of the axis displacement, this type of reflector has a natural hole in the middle of it that is not a defined part of the reflector surface. Thus when used as a true optical dual reflector, energy from the feed incident upon the subreflector does not optically reflect back into the feed, resulting in minimal feed to sub interaction. Figure 4 shows the profile and dimensions of both reflectors with respect to the feed horn location. The main reflector diameter of 108 inches was chosen to ensure meeting the required antenna gain at both C- and Ku-bands.

Additionally, this design utilizes both a true optical approach (Ku-band) hybridized with a rear radiating feed approach (C-band) [2]. For this coaxial design, at Ku-band the hollow center conductor illuminates the subreflector which in turn illuminates the main reflector. Sidelobe control and aperture efficiency are managed with the reflector shaping. At C-band, the rear radiation feed has been designed to efficiently radiate backwards into the reflector about a phase-ring which matches the main reflector focal-ring. In this case sidelobe control and efficiency are managed with intelligent design procedures.

The optical performance of the reflector system is predicted using a Body of Revolution (BOR) Method of Moments (MoM) simulation software package developed internally by the Harris team. This software accurately calculates radiation patterns due to the electromagnetic interaction of all of the surfaces shown in Figure 4. At C-band, the full optics were modeled in the BOR MoM code, while at Ku-band horn with subreflector patterns were computed and fed to GRASP [2] to generate secondary patterns.

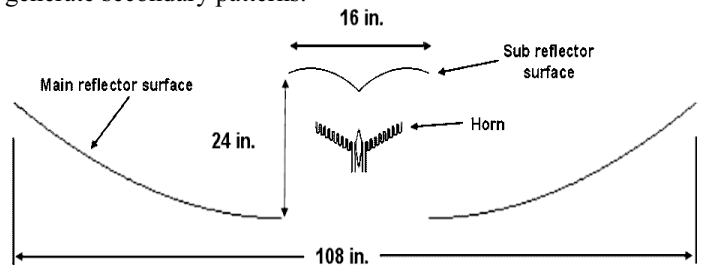


Figure 4 Dimensions of main and sub reflector with respect to feed horn

### B. Coaxial Waveguide Aperture

Many challenges are involved in the design of the dual band coaxial waveguide aperture. In addition to efficient dual-band illumination of the subreflector, matching and isolation are of key concern. In this design, the Ku-band circular waveguide is dielectrically loaded at the aperture, reducing the diameter of

the center conductor. This reduction in center conductor size leads to a coaxial waveguide geometry more suited to match C-band. In addition, the dielectrically loaded Ku-band aperture becomes more directive, improving isolation between Ku- and C-Bands. A three step impedance transformer is used in the coaxial waveguide to step from the C-band polarizer to the aperture. Additional matching features in the coaxial waveguide resulted in a C-band aperture match on the order of -20 dB. Aperture matching for the Ku-band is achieved by tapering into the dielectrically loaded circular waveguide section, and by utilizing a notch matching feature at the Ku aperture. A resulting Ku-band match on the order of -25dB was achieved via simulation. The Ku-band to C-band isolation for the aperture is less than -20 dB for all propagating Ku-band modes in the C-band coaxial waveguide.

The design work for the aperture was performed using a variety of analysis tools, including the Harris BOR-MoM tool, Ansoft HFSS, and MIG WASPNET. Figure 5 shows the geometry of the coaxial waveguide aperture.

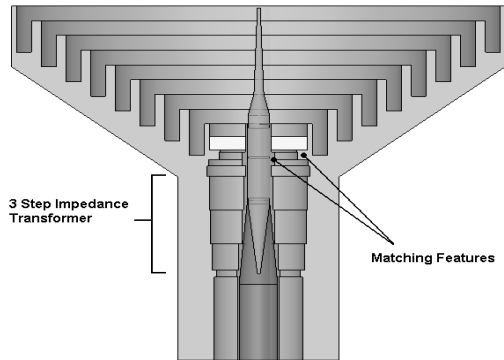


Figure 5 Geometry of the coaxial waveguide aperture

### C. C-band OMT

The coaxial waveguide C-band OMT design requirements are driven in part by the system level axial ratio requirement and the aperture return loss at C-band. In this feed topology, C-band aperture reflections propagate back through the polarizer and become cross polarized incident on the common port of the OMT. The OMT is designed to absorb this cross polarized signal in the transmit band, so that it does not reflect and re-radiate, degrading axial ratio. A corrugated waveguide low-pass filter is employed on the receive arm of the OMT to contain the transmit cross-polarized signal to the junction. Loaded symmetric rectangular waveguide arms are used to absorb the transmit-band cross polarized signal incident on the common port.

Design work was performed using the finite element analysis tool Ansoft HFSS. Both simulated and measured return loss proved to be better than 20 dB at both ports. The geometry of the C-band OMT is shown in Figure 6.

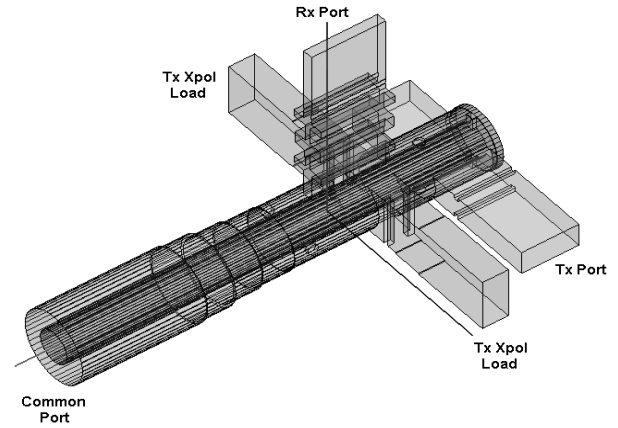


Figure 6 C-band coaxial waveguide OMT

### D. C-band Polarizer

The coaxial waveguide C-band polarizer design is based on a circular waveguide dielectric vane polarizer but is implemented in coaxial waveguide. The polarizer rotates on the propagation axis and can be set at three different angular positions to achieve the switchable circular, and linear polarization requirements. Coaxial waveguide choke joints at each end of the polarizer allow for the rotation of the outer conductor and dielectric vane components of the polarizer while the center conductor remains fixed. A compact design is achieved providing a component polarization axial ratio of less than 0.4 dB at transmit-band frequencies and less than 0.75 dB at receive-band frequencies. Such axial ratio was proved with both simulations and bench top measurements.

Design/analysis work was performed using Ansoft HFSS finite element tool. The geometry of the coaxial waveguide dielectric vane polarizer is shown in Figure 2.7

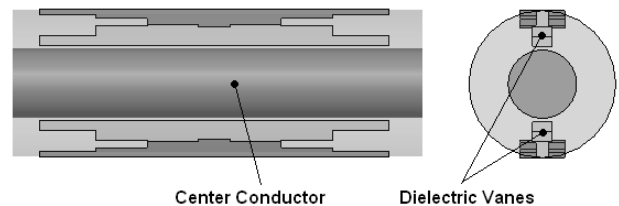


Figure 7 C-band coaxial waveguide dielectric vane polarizer configuration

## 3. MEASURED VS. PREDICTED DIRECTIVITY PATTERNS

In this section the antenna patterns are presented for the CBSP FLV antenna subsystem. The patterns were measured in a Spherical Near Field Range (SNFR) anechoic chamber made by MI Technologies. This type of antenna range scans an open-ended waveguide probe over a spherical surface enclosing the Antenna Under Test (AUT). The spherical surface can be in the near field of the AUT since far field data points are obtained through Fourier transforms and related

data processing [3]. Also, since the AUT is completely enclosed, directivity values are readily obtained through integration of the total power radiated.

Figure 8 shows a photograph of the AUT in the SNFR. The main reflector was pointed toward the chamber ceiling as the near field probe was scanned to all of the locations covering a complete sphere. The antenna was tested without a radome. The arc of the scan arm can be seen in the right hand side of the photograph. The AUT was tested at the transmit bands through the OMT ports as per the block diagram of Figure 1. At the receive ports filters were added between the receive OMT ports and the antenna range equipment so that the effects of such filters would appear in the pattern measurements. The filters are required by the terminal for out-of-band rejection and were needed during pattern testing since their effect on axial ratio could be significant if they produce multiple reflections within the feed. Figure 9 shows a photograph of the front of the reflector showing the sub reflector along with the feed enclosure.



Figure 8 The AUT as mounted in the SNFR prior to pattern testing

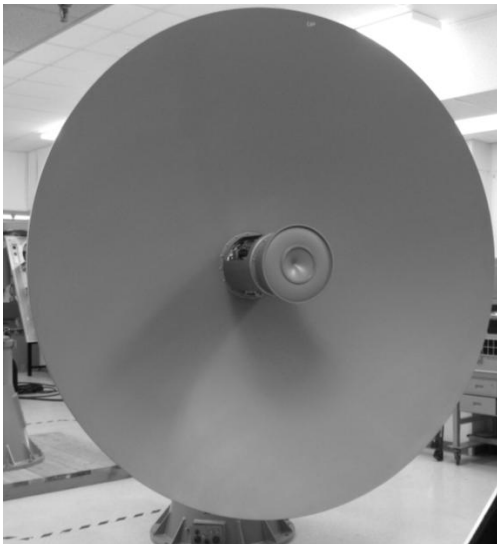
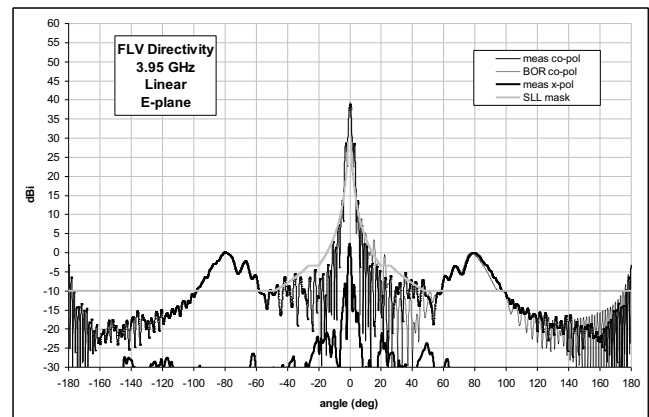


Figure 9 The AUT reflector and Feed

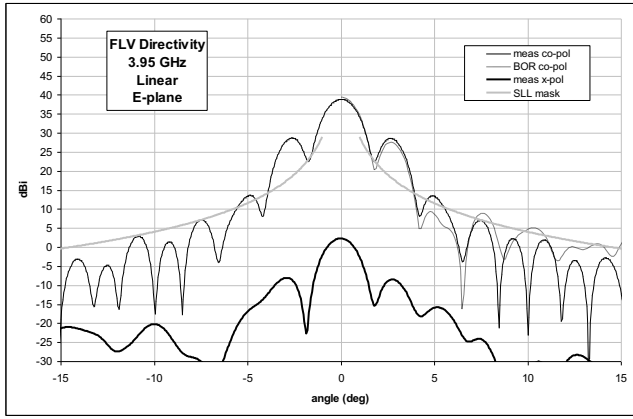
The patterns were measured at C-band with the C-band polarizer positioned for three co-polarization outputs: (1) Tx and Rx orthogonal linear polarization with results in Table 2 and Figure 10, (2) LHCP at Rx and RHCP at Tx with results in Table 3 and Figure 11, (3) RHCP at Rx and LHCP at Tx with results in Table 4 and Figure 12. At Ku-band only linear polarization was tested since only that polarization is capable by the feed and the Ku-band results are in Table 5 and Figure 13. Tables 2-5 list the measured directivity for all of the frequencies and polarization cases tested. The measured directivity values exceeded the required gain by .7 dB at C-band and 1.2 dB at Ku-band (worst case in band) to encompass feed losses. A complete feed loss budget will not be described further here. Also listed is the aperture efficiency and the polarization purity at beam peak. Cross-Polarization Discrimination (XPD) is listed for linear polarization and Axial Ratio (AR) is listed for the circular polarization cases. The measured Axial Ratio was better than .75 dB as per the requirement in Table 1.1. The measured aperture efficiencies were slightly below 60% at some frequencies most likely due to some pattern distortion due to the sub reflector support structure. Patterns were plotted at center-band only for brevity. The patterns show reasonable E-H plane symmetry, a desirable property, as can be seen in Figure 10 (e,f) and Figure 13 (e,f)

TABLE 2  
SUMMARY OF MEASURED DATA AT C-BAND WITH POLARIZER  
IN POSITION FOR LINEAR POLARIZATION

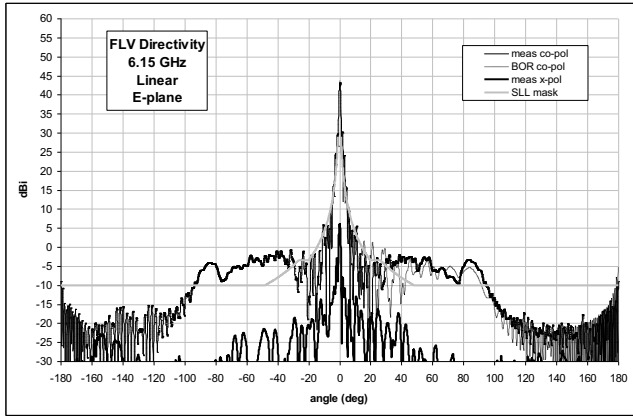
f (GHz)	band	polarization	co-pol dir (dBi)	ap eff (%)	XPD (dB)
3.700	Rx	V	38.7	65.8	33.8
3.750	Rx	V	39.0	68.1	35.2
3.800	Rx	V	39.2	69.6	36.5
3.850	Rx	V	39.2	67.9	32.2
3.900	Rx	V	39.0	63.6	33.4
3.950	Rx	V	38.9	60.2	36.6
4.000	Rx	V	38.8	57.9	38.6
4.050	Rx	V	39.2	61.5	42.2
4.100	Rx	V	39.3	62.0	34.3
4.150	Rx	V	39.4	61.9	33.1
4.200	Rx	V	39.6	62.8	37.9
5.850	Tx	H	42.8	68.2	35.7
5.900	Tx	H	42.7	65.3	37.1
5.950	Tx	H	42.7	63.3	38.0
6.000	Tx	H	43.1	69.0	38.7
6.050	Tx	H	43.4	71.8	37.9
6.125	Tx	H	43.1	66.0	36.8
6.150	Tx	H	43.1	65.8	37.2
6.200	Tx	H	43.2	66.0	37.4
6.250	Tx	H	43.1	63.6	38.4
6.350	Tx	H	43.2	63.4	38.1
6.425	Tx	H	43.4	64.4	34.4



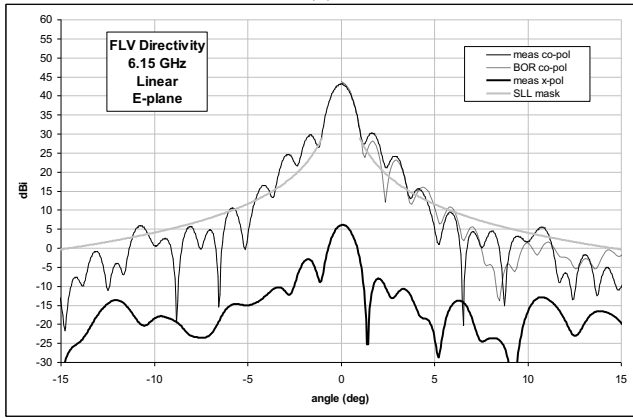
(a)



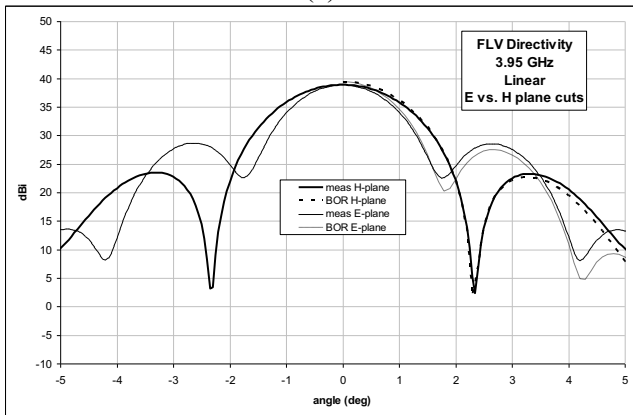
(b)



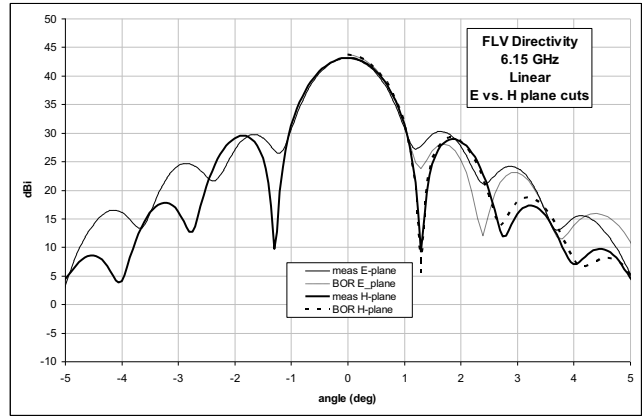
(c)



(d)



(e)

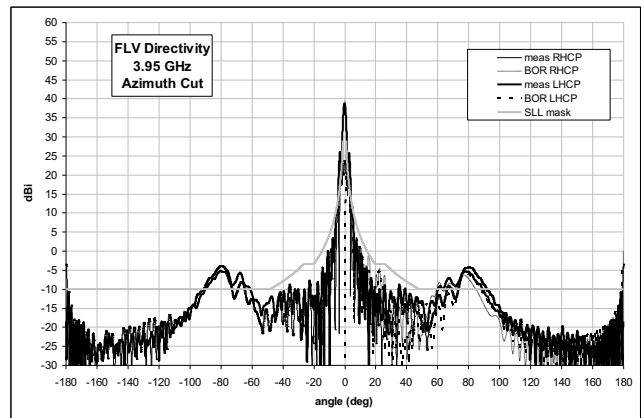


(f)

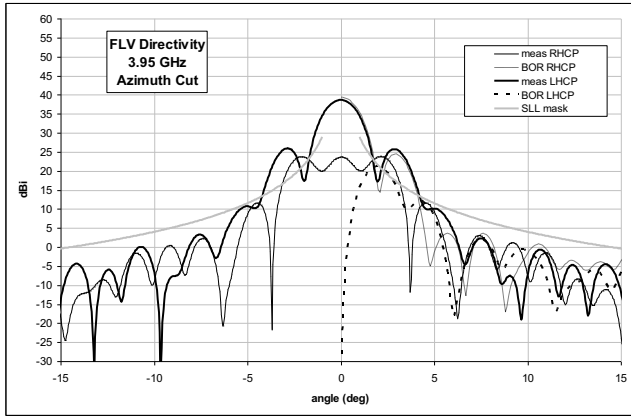
Figure 10 Measured Patterns of the feed with sub and main reflector at C-band for the linear polarization case. (a) 3.95 GHz, E-plane cut wide view. (b) 3.95 GHz, E-plane cut zoom view (c) 6.15 GHz E-plane cut wide view. (d) 6.15 GHz E-plane cut zoom view (e) 3.95 GHz E vs H-plane. (f) 6.15 GHz E vs H-plane.

TABLE 3  
SUMMARY OF MEASURED DATA AT C-BAND WITH POLARIZER  
IN POSITION FOR LHCP AT RX AND RHCP AT TX

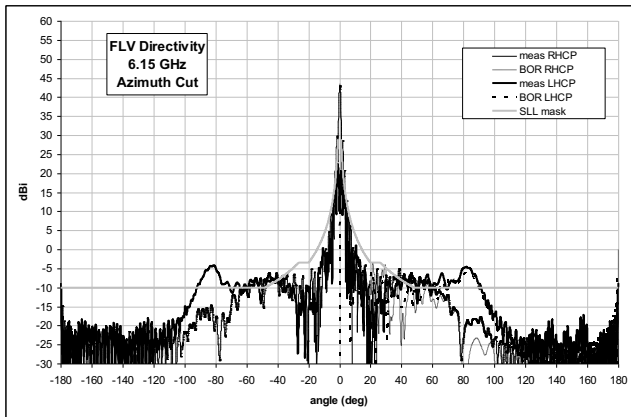
f (GHz)	band	polarization	co-pol dir (dBi)	ap eff (%)	AR (dB)
3.700	Rx	LHCP	38.6	64.1	1.2
3.750	Rx	LHCP	38.9	67.1	0.3
3.800	Rx	LHCP	39.1	69.0	0.7
3.850	Rx	LHCP	39.1	66.6	1.6
3.900	Rx	LHCP	38.8	60.4	2.9
3.950	Rx	LHCP	38.6	56.8	3.1
4.000	Rx	LHCP	38.7	56.2	2.1
4.050	Rx	LHCP	39.1	60.0	1.2
4.100	Rx	LHCP	39.2	59.4	1.8
4.150	Rx	LHCP	39.3	59.7	1.3
4.200	Rx	LHCP	39.5	61.4	0.4
5.850	Tx	RHCP	42.8	67.0	0.4
5.900	Tx	RHCP	42.7	64.5	0.6
5.950	Tx	RHCP	42.6	62.8	0.5
6.000	Tx	RHCP	43.1	68.7	0.4
6.050	Tx	RHCP	43.3	71.0	0.5
6.125	Tx	RHCP	43.1	65.4	0.3
6.150	Tx	RHCP	43.1	65.2	0.4
6.200	Tx	RHCP	43.2	65.3	0.6
6.250	Tx	RHCP	43.1	63.0	0.5
6.350	Tx	RHCP	43.2	62.6	0.3
6.425	Tx	RHCP	43.4	64.0	0.7



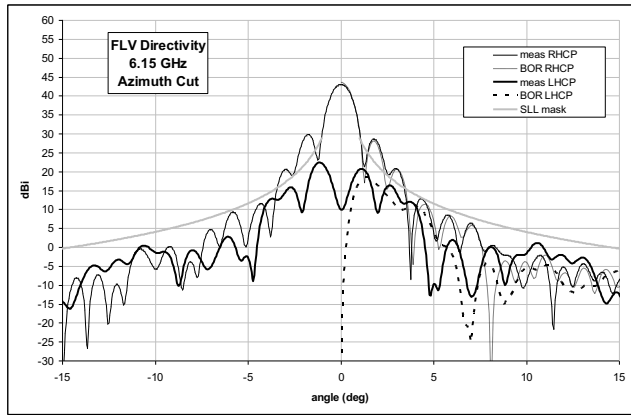
(a)



(b)



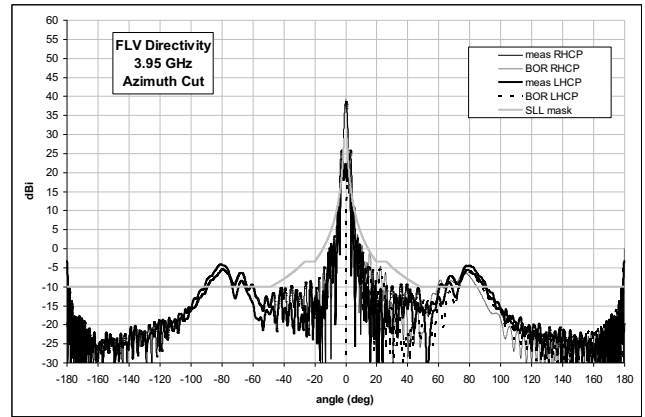
(c)



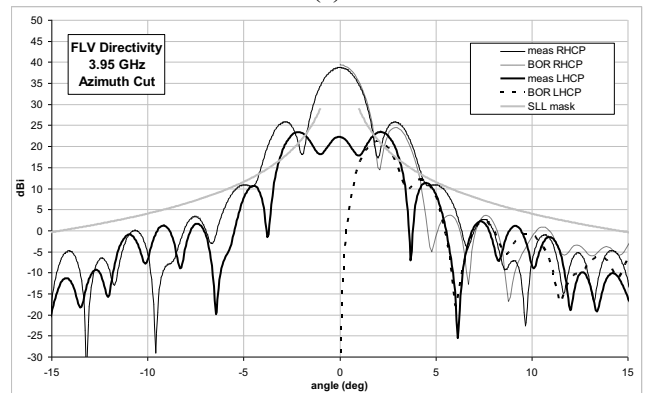
(d)

TABLE 4  
SUMMARY OF MEASURED DATA AT C-BAND WITH POLARIZER  
IN POSITION FOR RHCP AT RX AND LHCP AT TX

f (GHz)	band	polarization	co-pol dir (dBi)	ap eff (%)	AR (dB)
3.700	Rx	RHCP	38.7	65.4	0.6
3.750	Rx	RHCP	38.9	67.4	0.4
3.800	Rx	RHCP	39.1	68.4	0.9
3.850	Rx	RHCP	39.1	65.8	2.4
3.900	Rx	RHCP	38.9	62.1	2.3
3.950	Rx	RHCP	38.8	58.3	2.6
4.000	Rx	RHCP	38.6	55.4	2.6
4.050	Rx	RHCP	39.0	58.9	1.3
4.100	Rx	RHCP	39.2	60.1	1.3
4.150	Rx	RHCP	39.4	60.6	1.5
4.200	Rx	RHCP	39.5	61.9	1.0
5.850	Tx	LHCP	42.8	67.1	0.6
5.900	Tx	LHCP	42.7	64.3	0.5
5.950	Tx	LHCP	42.6	62.8	0.4
6.000	Tx	LHCP	43.1	68.5	0.4
6.050	Tx	LHCP	43.3	71.0	0.2
6.125	Tx	LHCP	43.0	65.2	0.5
6.150	Tx	LHCP	43.1	64.9	0.4
6.200	Tx	LHCP	43.2	65.2	0.1
6.250	Tx	LHCP	43.1	62.9	0.4
6.350	Tx	LHCP	43.2	62.6	0.4
6.425	Tx	LHCP	43.4	63.5	0.6

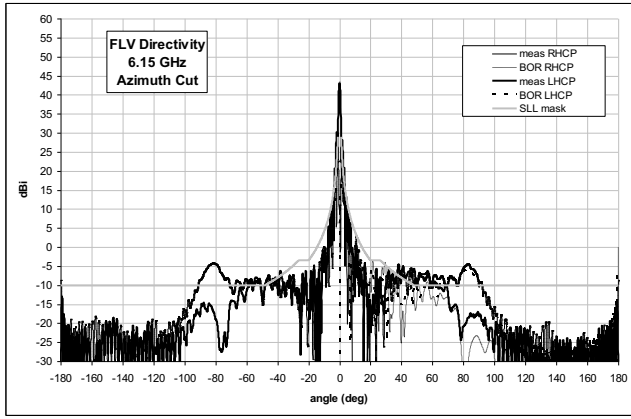


(a)

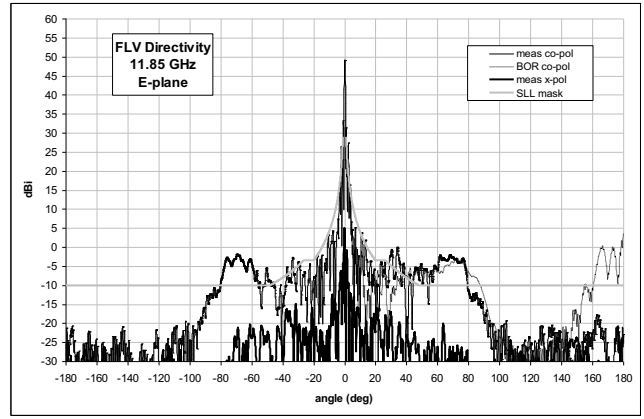


(b)

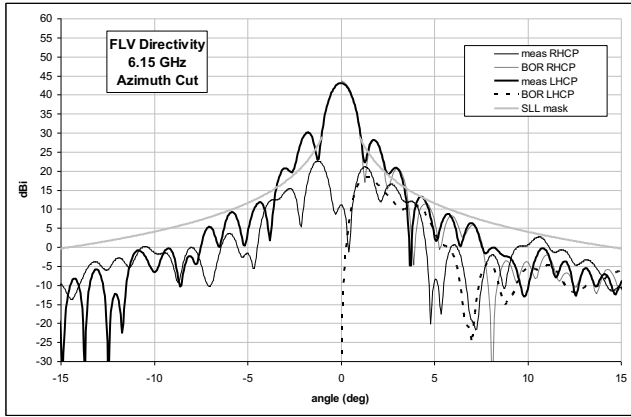
Figure 11 Measured Patterns of the feed with sub and main reflector at C-band with polarizer in position for LHCP at Rx and RHCP at Tx. (a) 3.95 GHz, wide view. (b) 3.95 GHz, zoom view (c) 6.15 GHz wide view. (d) 6.15 GHz zoom view.



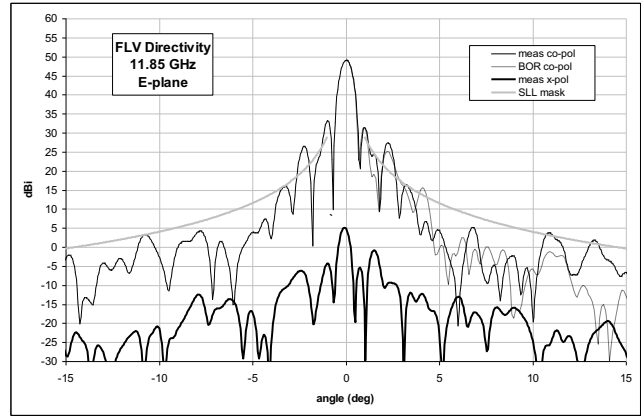
(c)



(a)



(d)



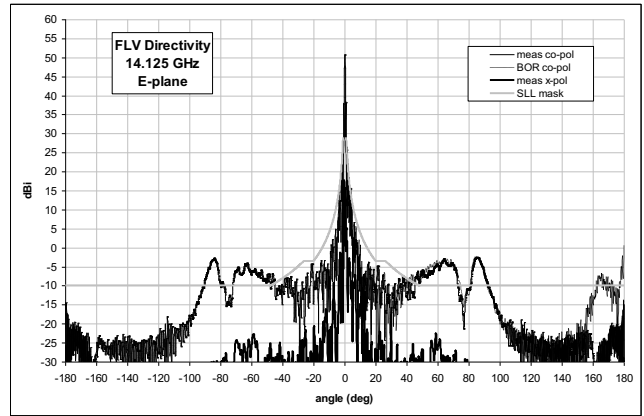
(b)

Figure 12 Measured Patterns of the feed with sub and main reflector at C-band with polarizer in position for RHCP at Rx and LHCP at Tx. (a) 3.95 GHz, wide view. (b) 3.95 GHz, zoom view (c) 6.15 GHz wide view. (d) 6.15 GHz zoom view.

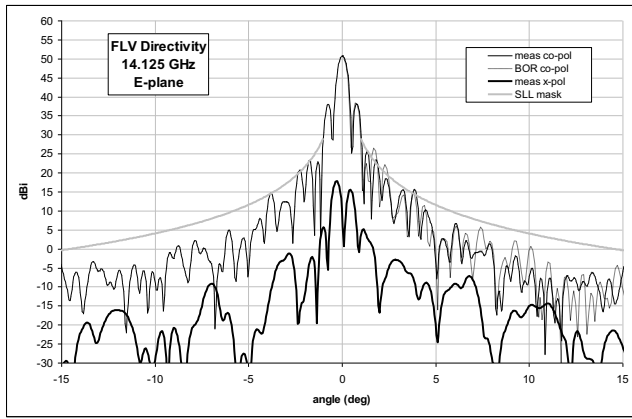
TABLE 5

SUMMARY OF MEASURED DATA AT KU-BAND

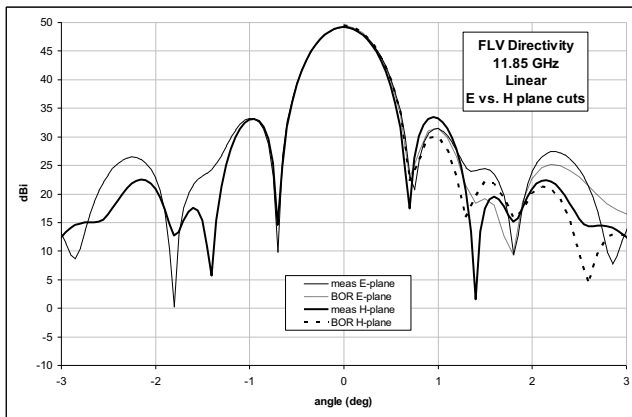
f (GHz)	band	polarization	co-pol dir (dBi)	ap eff (%)	XPD (dB)
10.950	Rx	V	48.4	69.1	42.3
11.150	Rx	V	48.5	69.3	38.1
11.300	Rx	V	48.7	70.0	41.7
11.550	Rx	V	48.8	69.3	39.9
11.850	Rx	V	49.1	70.8	44.3
12.000	Rx	V	49.2	69.8	43.6
12.200	Rx	V	49.4	70.8	38.0
12.400	Rx	V	49.6	71.6	45.0
12.600	Rx	V	49.7	70.7	37.8
12.750	Rx	V	49.7	69.8	38.5
13.750	Tx	H	50.9	78.2	41.1
13.900	Tx	H	50.8	74.6	40.9
14.000	Tx	H	50.7	73.1	39.7
14.050	Tx	H	50.7	71.9	39.6
14.125	Tx	H	50.8	72.8	40.5
14.175	Tx	H	50.9	73.7	40.1
14.200	Tx	H	50.9	73.9	38.2
14.300	Tx	H	50.9	73.6	37.8
14.400	Tx	H	50.7	69.4	42.1
14.500	Tx	H	50.8	69.5	44.5



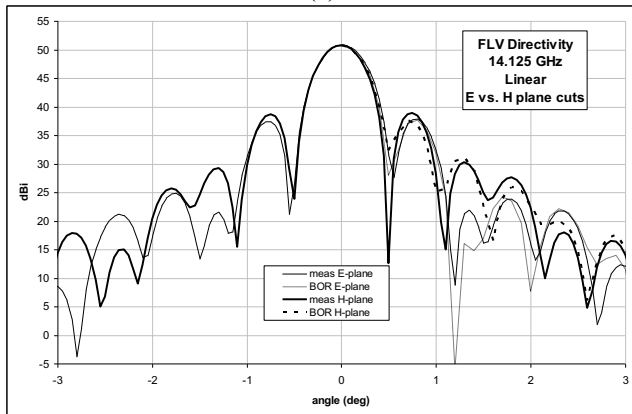
(c)



(d)



(e)



(f)

Figure 13 Measured Patterns of the feed with sub and main reflector at Ku-band. (a) 11.85 GHz, H-plane cut wide view. (b) 11.85 GHz, H-plane cut zoom view (c) 14.125 GHz E-plane cut wide view. (d) 14.125 GHz E-plane cut zoom view (e) 11.85 GHz E vs H-plane. (f) 14.125 GHz E vs H-plane

#### 4. CONCLUSIONS

A 108” simultaneous C/Ku band antenna subsystem was designed and tested to successfully operate from 3.7 to 14.5 GHz. This antenna not only offers dual band capability but also multiple polarizations at both transmit and receive. The use of a single feed and simultaneous operation results in a

terminal that does not require feed swapping, a customer desired feature.

There were some non-compliances to the antenna requirements as initially flowed down to the antenna subsystem. For example the aperture efficiency requirement of 65% as per Table 1.1 was not met at all frequencies tested. At 4.0 GHz an aperture efficiency of 55.4% was measured (Table 3.3), however through additional system analysis this efficiency proved to have minimal impact on the overall system throughput. In addition, not all side-lobes met the requirement of [1] as can be seen in measured patterns of Figures 3.3-3.6. The antenna patterns were however customer approved.

The design of the antenna was achieved through the use of many commercially available electromagnetic analysis and design tools. The use of such tools yielded a design that did not require costly iterations to the prototype waveguide components and prototype reflector design.

#### 5. REFERENCES

- [1] Department of Defense Interface Standard, MIL-STD188-164A w/ change 2, “Interoperability of SHF Satellite Communications Earth Terminals,” 2004
- [2] G. Gothard et al, “DESIGN OF A SIMULTANEOUS CENTER-FED X/KA-BAND SATCOM REFLECTOR ANTENNA WITH REPLACABLE C-BAND OPTION,” *MilCom*, 2007
- [3] D. W. Hess, “The IsoFiltertrade technique: isolating an individual radiator from spherical near-field data measured in a contaminated environment,” *The Second European Conference on Antennas and Propagation*, 2007. *EuCAP 2007*